JOURNAL OF COMPUTATIONAL PHYSICS 105, 1–13 (1993)

Nonconservative Hybrid Shock Capturing Schemes

EDUARD HARABETIAN*

Department of Mathematics, University of Michigan, Ann Arbor, Michigan 48109

AND

ROBERT PEGO†

Department of Mathematics, University of Maryland, College Park, Maryland 20742

Received January 27, 1991; revised May 7, 1992

We examine some efficient numerical approximations for hyperbolic systems of conservation laws. The approximations are constructed by hybridizing simple, accurate centered difference schemes (for use in smooth regions), with sophisticated shock capturing schemes (for use only in narrow zones near shocks and other singularities). The switching strategies we consider are very flexible in allowing one to choose schemes independently for different regions of the flow. The resulting hybrid schemes need not be conservative. But numerical examples in one dimension demonstrate that if the switching strategy is cautious (e.g., if switching is prohibited too close to shocks), then high accuracy can be achieved for both shock speeds and smooth regions. For one switching strategy in particular it is easy to prove convergence to the entropy solution.

1. INTRODUCTION

In this paper we consider numerical schemes for systems of conservation laws of the form

$$u_t + f(u)_x = 0. \tag{1}$$

Solutions of (1) typically develop discontinuities, for which standard formally high order accurate schemes based on centered differencing produce ruinous oscillations and unphysical solutions. Conservation-form schemes which approximate shocks well without oscillations are hard to design for high accuracy in smooth regions. In recent years a number of successful schemes (e.g., TVD and ENO schemes) have been designed which in practice exhibit desirable properties such as: narrow numerical shock zones without overshoots or undershoots; formal high order accuracy in smooth regions; and convergence to the physically correct discontinuities satisfying an entropy condition (cf. [9, 11, 16, 18, 5, 10]). But while these sophisticated schemes work well near shocks, they pay a performance penalty, since their shock-handling features are used everywhere in the grid. Especially expensive are the field-by-field decompositions computed at each point in order to obtain upwind differencing.

A natural approach to improving efficiency is hybridization: Use a cheap, accurate centered difference scheme in smooth regions, and switch to a sophisticated shock-capturing scheme near discontinuities. Many of the schemes mentioned above incorporate a hybrid principle in their design, in order to obtain stability near shocks and accuracy away from shocks. By and large, however, efficiency remains difficult to achieve for accurate schemes in conservation form. It is comparatively easy to design an efficient nonconservative hybrid—one can switch between completely different schemes at adjacent points on the grid. But past experience and theory have indicated that such nonconservative hybrids produce poor approximations to weak solutions, usually yielding errors in shock speeds of the order of 10% (cf. [20, 21]).

Here we propose that an appropriate choice of *switching strategy* can overcome this problem in nonconservative hybrids. We find that if switching between schemes is minimized, and not permitted in shock zones (where conservation form remains important), good performance can be achieved with great flexibility in the choice of schemes and the hybrid design. A key idea is to distinguish between *detecting* and *defining* shock zones. Shocks (and other singularities) are detected when a smoothness indicator exceeds some threshold value. But simple indicators often vary above and below threshold in an irregular pattern near a single shock. It makes sense to smooth this pattern in

* Research supported by NSF Grants DMS-8801991 and DMS-9003965.

† Research supported by NSF Grants DMS-8807032 and DMS-8902422, and by the Institute for Physical Science and Technology, University of Maryland.

0021-9991/93 $5.00

order to define the shock zone. Moreover, a cheap scheme may have a wide stencil, rendering it inaccurate (or untrustworthy) within a certain distance from the shock. This suggests that the shock zone, defined as the zone in which the good shock-capturing scheme is used, should be sufficiently broad so that switching occurs where both schemes are performing well.

Based on the ideas above, in this paper we describe some simple ways of combining existing schemes, in order to achieve efficiency and accuracy in smooth regions, while retaining stability and resolution in shock zones. We describe a number of such schemes that perform well on test problems in one dimension and note that the concepts can be easily extended to the multidimensional case, where the efficiency considerations are expected to be most relevant.

For example, in Section 2.3 we describe a scheme, which, in smooth regions, uses fourth-order centered differences in space and the Runge–Kutta method in time. This part of the comptation can be vectorized, and the time step can be taken twice as large as is usually possible. (The maximum CFL number for linear stability of this scheme is about twice that of many traditional schemes.) In the shock zone, the values from this cheap scheme are simply discarded, and an appropriate upwind method is used. The upwind scheme may be difficult or impossible to vectorize, but it need only be computed at the relatively few points in the shock zone. We give several numerical examples to show that this hybrid can achieve high accuracy in smooth regions while computing accurate shock speeds with the same resolution as the upwind scheme, despite the lack of perfect conservation form.

Another nonconservative hybridizing strategy that performs well is described in Section 2.4. In smooth regions, we start with a semidiscrete scheme that uses fourth-order centered differences in space and is continuous in time. In shock zones, this scheme is replaced by a flux-based fourth-order ENO scheme of Shu and Osher [18], which is also continuous in time. The resulting combined scheme is discretized in time using a Runge–Kutta method. In this approach, the programming difficulty in constructing a hybrid is reduced, since the same time discretization is done for both component schemes; also, significant components of the computation should be vectorizable.

The ideas developed here can also be applied to obtain some efficient hybrid schemes in conservation form. In Section 3 we show how to modify the Shu–Osher ENO scheme to build a semidiscrete conservative hybrid which uses simple fourth-order centered differences in smooth regions while retaining full fourth-order accuracy when switching occurs.

A traditional method of efficiently computing flows with shocks is to modify a simple higher order accurate conservative scheme to include sufficient dissipation that undesirable overshoots in shocks are eliminated and unphysical shocks prevented. In the large scale computations of Jameson [13], dissipation is carefully added in conservation form in a hand-tuned, solution-specific fashion near shocks only, leaving the basic fast second-order scheme undisturbed in smooth regions. Field-by-field decompositions are not required at all in this approach. A different approach to improving efficiency has been suggested by Engquist *et al.* [8]. These authors introduce conservative nonlinear filters to postprocess at each time step the result of using a high-order-accurate centered scheme. The filters are designed simply to obtain an oscillation-free solution. In practice they are activated only in shock zones, so field-by-field decompositions can be avoided in most of the grid.

2. NONCONSERVATIVE SWITCHING STRATEGIES

In this section, we describe four nonconservative hybridizing strategies, ranging from a very simple strategy for which a convergence result can be proved, to more practical and efficient strategies. All the hybrid schemes we present update the solution at each grid point by making a simple choice between two schemes (or among several). The differences lie in the selection of component schemes to hybridize, and the switching strategy used to make the choice at each grid point.

The first two strategies we present basically rely on truncation error estimates obtained by comparing different schemes. Recognizing that such error estimates essentially serve to *detect* shocks, but perform badly when used pointwise to define shock zones, we are led to construct a switching strategy based on a rather simple shock zone detection/definition algorithm. This algorithm amounts to detecting shocks by using a smoothness indicator, and then defining the shock zone to include any grid point where the smoothness indicator fails, plus a buffer zone of a few grid points on either side.

We describe and test two hybrid schemes based on this strategy, a fully discrete hybrid and a semidiscrete one. The latter has the advantage that it is easier to program in combination with a high order accurate ENO scheme. The numerical tests aim to show that shock speeds can be computed accurately, while using a cheap, accurate scheme in smooth regions, despite the fact that the hybrid scheme overall is not in conservation form.

2.1. *Simple Hybrids*

Suppose u is a scalar. Given grid increments Δx and Δt, u_j^n denotes an approximation to $u(j\,\Delta x, n\,\Delta t)$. A one-step scheme may be denoted by $u_j^{n+1} = G(u^n)_j$. Given two schemes G_0 and G_1, a very simple nonconservative hybrid scheme G_H can be constructed as follows: At time level n,

determine switches $s_j(u^n)$ (with values 0 or 1) and define the hybrid scheme by

$$u_j^{n+1} = G_H(u^n)_j = \begin{cases} G_0(u^n)_j & \text{if} \quad s_j = 0 \\ G_1(u^n)_j & \text{if} \quad s_j = 1. \end{cases} \tag{2}$$

The hybrid is determined by the choice of the schemes G_0 and G_1, together with the switching strategy. A class of simple hybrids which can be shown to converge to the entropy solution arise when G_1 is a monotone scheme, G_0 is arbitrary (it may not even be a one step scheme), and the switching strategy guarantees that the hybrid is a small perturbation of G_1. For example, the switches can be determined as follows: Let r be a positive function such that $r(\Delta x) \to 0$ as $\Delta x \to 0$, and choose

$$s_j = \begin{cases} 0 & \text{if} \quad |G_0(u^n)_j - G_1(u^n)_j| \leqslant \Delta t\, r(\Delta x), \\ 1 & \text{if} \quad |G_0(u^n)_j - G_1(u^n)_j| > \Delta t\, r(\Delta x). \end{cases} \tag{3}$$

That is, $s_j = 0$ if G_0 and G_1 "agree" at grid point j, and $s_j = 1$ if they "disagree." Then $G_H(u^n)_j = G_0(u^n)_j + s_j(G_1(u^n)_j - G_0(u^n)_j)$, and we have

$$|G_H(u^n)_j - G_1(u^n)_j| \leqslant \Delta t\, r(\Delta x). \tag{4}$$

For this class of simple hybrids, we have

THEOREM 1. *Assume that the monotone scheme G_1 has a finite stencil of width $2P+1$, i.e.,*

$$G_1(u)_k = G_1(v)_k \qquad \text{if} \quad u_j = v_j \text{ for } |k-j| \leqslant P.$$

Assume $\Delta t/\Delta x \geqslant c_0 > 0$. Let u_j^n be determined by (2) *and* (3) *above, and let v_j^n be a solution obtained by the monotone scheme alone, so that $v_j^{n+1} = G_1(v^n)_j$. Then so long as $n\,\Delta t \leqslant T$ and $(2q+1)\,\Delta x \leqslant L$, we have*

$$\sum_{|j| \leqslant q} |u_j^n - v_j^n|\,\Delta x \leqslant \sum_{|j| \leqslant q + nP} |u_j^0 - v_j^0|\,\Delta x + C(T, L)\, r(\Delta x), \tag{5}$$

where $C(T, L) = (L + 2PT/c_0)T$.

Proof. By (4) we have

$$\begin{aligned} \sum_{|j| \leqslant q} |u_j^n - v_j^n|\,\Delta x &= \sum_{|j| \leqslant q} |G_H(u^{n-1})_j - G_1(v^{n-1})_j|\,\Delta x \\ &\leqslant \sum_{|j| \leqslant q} |G_1(u^{n-1})_j - G_1(v^{n-1})_j|\,\Delta x \\ &\quad + \Delta t\, \kappa(\Delta x)(2q+1)\,\Delta x. \end{aligned}$$

Define $\tilde{u}_j^{n-1} = u_j^{n-1}$ for $|j| \leqslant q+P$, $=0$ for $|j| > q+P$, and similarly define $\tilde{v}_j^{n-1}$. Then $G_1(u^{n-1})_j = G_1(\tilde{u}^{n-1})_j$ for $|j| \leqslant q$, and similarly for v, so since G_1 is an l_1-contraction [7], we have

$$\begin{aligned} &\sum_{|j| \leqslant q} |G_1(u^{n-1})_j - G_1(v^{n-1})_j|\,\Delta x \\ &\quad \leqslant \sum_j |G_1(\tilde{u}^{n-1})_j - G_1(\tilde{v}^{n-1})_j|\,\Delta x \\ &\quad \leqslant \sum_j |\tilde{u}_j^{n-1} - \tilde{v}_j^{n-1}|\,\Delta x \\ &\quad = \sum_{|j| \leqslant q+P} |u_j^{n-1} - v_j^{n-1}|\,\Delta x. \end{aligned}$$

By induction the estimate (5) follows.

Closely related to this result are remarks of Shu and Osher [18], who describe some "essentially conservative" ENO schemes which differ from the Lax–Friedrichs scheme by $O(\Delta x^2)$. Shu and Osher remark that such schemes yield every convergence property that the monotone scheme has, full convergence in multidimensional scalar problems to solutions satisfying the entropy condition. More precisely, our Theorem 1, which may be easily extended to the multidimensional case, yields convergence of the hybrid to the entropy solution in L^1_{loc}.

Also highly relevant is the work of Cockburn [3]. (See also LeRoux [14].) In [3], Cockburn describes how to combine numerical fluxes for two conservative schemes, the first an arbitrary three-point monotone scheme and the second scheme arbitrary, in order to obtain a "quasimonotone" scheme which is proved to be TVD and convergent to the entropy solution. Cockburn shows that if the numerical fluxes coincide with the Gudonov and Lax–Wendroff respectively to two terms in a Taylor expansion, then formally the quasimonotone flux will agree with the second flux, in smooth regions, where $x \mapsto f(u(x, t))$ is monotone; hence the combined scheme will retain the full accuracy of the second scheme.

2.2. *Variable Order*

At a practical level, the switching strategy in (3) is not very successful. When the tolerance is sufficiently stringent, shock speeds *are* in fact computed correctly, and the large errors traditionally associated with nonconservative schemes are avoided. But in practice, one wants to use G_0, typically a cheap, higher-order accurate scheme, for accuracy in smooth regions. Then one should choose the tolerance $\Delta t r(\Delta x)$ to be larger than $O(\Delta x^2)$, the truncation error of the monotone scheme. If the tolerance is too lax, switching may occur in the shock zone, creating larger errors in conservation which lead to incorrect shock speeds. In choosing the tolerance, there is a delicate balance which can be difficult to achieve. In the course of a computation,

a tolerance large enough to permit the use of G_0 in smooth regions may be too lax to correctly track a weak shock.

Performance may be improved by a more sophisticated switching strategy. One may argue that the high order accurate scheme should be used only when justifiable, e.g., when an estimate of truncation error indicates that the scheme is performing at its designed accuracy. The test in (3) accepts the high order scheme too readily, rejecting it only when it performs worse than a first-order accurate scheme. This leads one to consider "variable order" hybrids, with switching based on truncation error estimates, while making sure that an estimate like (4) holds to guarantee correct entropy production.

Let us now consider in detail such a variable order strategy, while noting that the switching strategies to be discussed in Sections 2.3 and 2.4 are probably more practical. We will switch among the following schemes: Let G_{LF} = Lax–Friedrichs scheme (a cheap monotone scheme), G_{EO} = second-order Engquist–Osher scheme (or any higher quality shock capturing scheme), G_{LW} = Lax–Wendroff (a cheap second-order scheme), G_{RK4}, G_{RK5} = fourth-order centered differences in space, with fourth- and fifth-order Runge–Kutta–Fehlberg time discretization, respectively. We argue as follows, to determine which scheme to use at any given grid point. Part of our motivation is to minimize the use and computation of the expensive shock capturing scheme: First compute the cheap schemes G_{LF}, G_{LW}, G_{RK4}, and G_{RK5} everywhere in the grid. Now at each grid point, compare G_{LF} and G_{LW}. If they disagree at first order in the grid size, a shock zone is detected. There we will choose the scheme G_{EO}. If G_{LF} and G_{LW} agree, compare G_{LW} and G_{RK4} at second order. If these disagree, this is a reason to believe that the use of a cheap accurate scheme is not justified, so again we choose G_{EO}. If G_{LW} and G_{RK4} agree, then compare G_{RK4} and G_{RK5}. (The difference is the estimate of the time truncation error of G_{RK4} produced by the RKF45 method.) If these agree at fourth order, use G_{RK4}. Otherwise, use of a fourth-order scheme is not justified, but use of the cheap second-order scheme G_{LW} is, so choose that.

In order to define the scheme precisely, let C_1, C_2, C_3 be constants and define the switches:

$$s_{1j} = \begin{cases} 0 & \text{if } |G_{\mathrm{LF}}(u^n)_j - G_{\mathrm{LW}}(u^n)_j| \leqslant C_1\,\Delta x^2 \\ 1 & \text{if } |G_{\mathrm{LF}}(u^n)_j - G_{\mathrm{LW}}(u^n)_j| > C_1\,\Delta x^2 \end{cases} \tag{6}$$

$$s_{2j} = \begin{cases} 0 & \text{if } |G_{\mathrm{LW}}(u^n)_j - G_{\mathrm{RK4}}(u^n)_j| \leqslant C_2\,\Delta x^3 \\ 1 & \text{if } |G_{\mathrm{LW}}(u^n)_j - G_{\mathrm{RK4}}(u^n)_j| > C_2\,\Delta x^3 \end{cases} \tag{7}$$

$$s_{3j} = \begin{cases} 0 & \text{if } |G_{\mathrm{RK5}}(u^n)_j - G_{\mathrm{RK4}}(u^n)_j| \leqslant C_3\,\Delta x^5 \\ 1 & \text{if } |G_{\mathrm{RK5}}(u^n)_j - G_{\mathrm{RK4}}(u^n)_j| > C_3\,\Delta x^5 \end{cases} \tag{8}$$

The variable order hybrid scheme G_H is defined by

$$\begin{aligned} G_H(u^n)_j = {} & (1-s_{1j})(1-s_{2j})(1-s_{3j})\,G_{\mathrm{RK4}}(u^n)_j \\ & + (1-s_{1j})(1-s_{2j})\,s_{3j}G_{\mathrm{LW}}(u^n)_j \\ & + (s_{1j}+s_{2j}-s_{1j}s_{2j})\,G_{\mathrm{EO}}(u^n)_j \end{aligned} \tag{9}$$

This switching strategy ought to detect the different kinds of singularities in the flow (shocks, rarefaction corners, etc.) and choose between the expensive scheme G_{EO} and one of the cheap schemes of "best" order in that region. Only when difficult singularities are detected is it necessary to compute the expensive scheme since only cheap schemes are used in computing the switches. Since shock zones are only a small region of a typical flow, this should be a cost-effective strategy, especially for systems where field-by-field decompositions are part of any sophisticated upwind scheme.

EXAMPLE 1. We consider the inviscid Burgers equation,

$$u_t + \left(\frac{u^2}{2}\right)_x = 0$$

in the interval $[-1, 1]$ with periodic boundary conditions and initial data given by

$$u_0(x) = x - \frac{0.9}{2\pi}\sin(2\pi x) + 1. \tag{10}$$

The solution exhibits a shock moving at constant speed $s = 1$ and a "feature," i.e., a smooth region where higher derivatives become rather large. We seek to compute the solution at time $t = 2.5$. Compared to the standard shock formation problem in Example 8 below, this problem is somewhat more challenging, since the shock travels more than a full spatial period, and a high order accurate scheme is needed to resolve the "feature." (Compare Fig. 3b.)

To compute the solution we use the variable order hybrid described above with $G_{\mathrm{RK4}}(u^n)_j$ replaced by $G_{\mathrm{RK4}}(u^n)_j - C_4\,\Delta t(\Delta^4 u)_j$, where $\Delta^4 u$ is the fourth difference operator in space. Without the fourth-order dissipation term the scheme $G_{\mathrm{RK4}}(u^n)_j$ tends to propagate the large errors produced in the neighborhood of the shock with a speed smaller than that of the shock and this causes the entire region behind the shock to be polluted. The fourth-order dissipation effectively eliminates this propagation of error in the scalar test problems.

We chose $C_1 = C_2 = C_3 = 5$ and $C_4 = 1$ and CFL # $= 0.8$. The computation used 80 mesh points and the results are shown in Fig. 1 at time $t = 2.5$. The solid line in Fig. 1a represents the exact solution which was computed from the formula $u(x, t) = u_0(a)$, where a satisfies

$$x - tu_0(a) = a \tag{11}$$

and we solved for a with a bisection method.

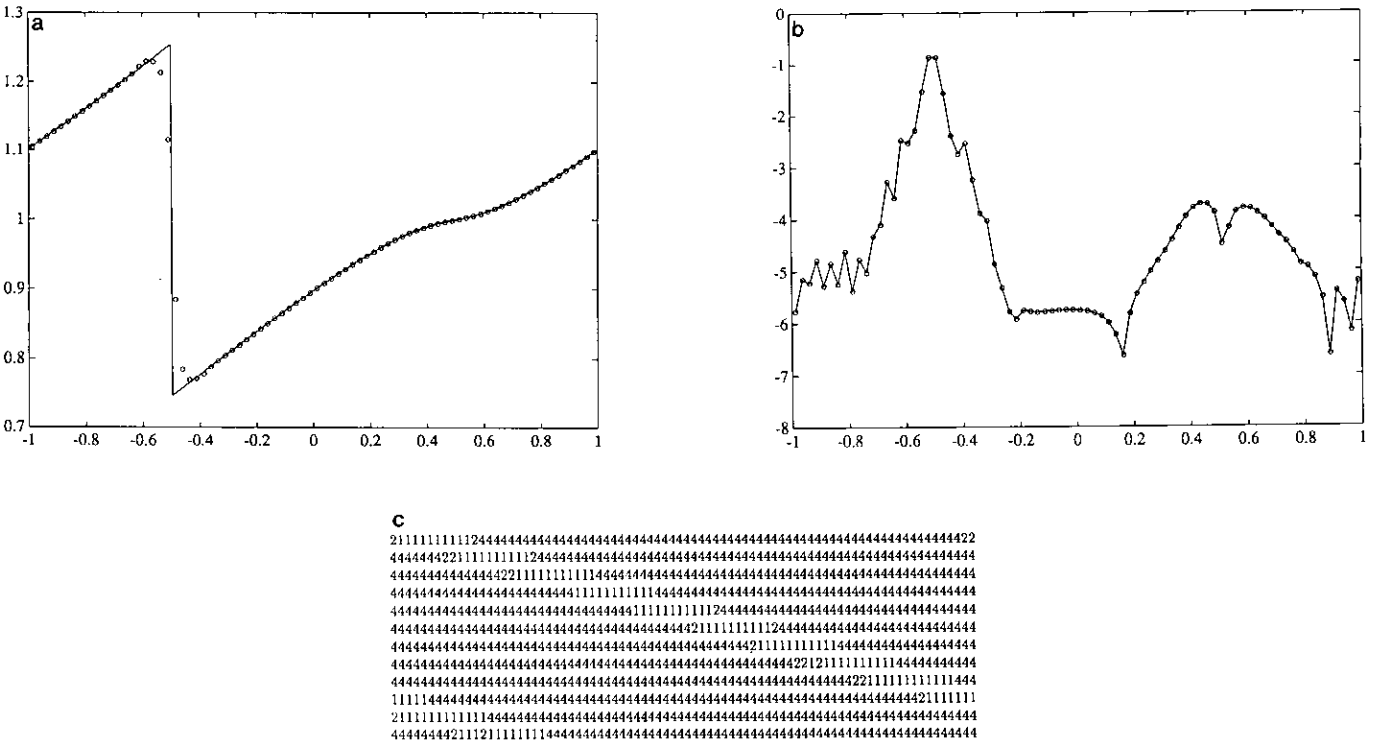

FIG. 1. Shock with a feature for Burgers' equation, computed with the variable order hybrid of Example 1: (a) Computed solution u_j and exact solution u, at $t = 2.5$. (b) $\log_{10} |u_j - u(x_j)|$ at $t = 2.5$. (c) Schemes used at x_j for every 20th time step: 1 = second-order Engquist–Osher; 2 = Lax–Wendroff; 4 = centered in x-RKF45 in t.

In Fig. 1b we plot the base 10 log of the absolute value of the error. In Fig. 1c we show the schemes used at each grid point for every 20 time steps, where $1 = G_{\mathrm{EO}}$, $2 = G_{\mathrm{LW}}$, $4 = G_{\mathrm{RK4}}$. We note that the points where the Lax–Wendroff scheme was used act as a buffer between the shock zone where the upwind scheme was used and the smooth region where the fourth-order centered scheme was used. It seems that G_{RK4}, which has a very wide stencil, fails the truncation error test in the immediate neighborhood of the shock zone. However, this region is smooth enough for the second-order Lax–Wendroff scheme.

EXAMPLE 2. We consider the non-convex conservation law (see Sanders [16]),

$$u_t + \left(\frac{4u^2}{4u^2 + (1-u)^2} \right)_x = 0$$

in the interval $[-1, 1]$, with periodic boundary conditions and initial data given by

$$u(x, 0) = \begin{cases} 1 & \text{if } -0.5 < x < 0, \\ 0 & \text{otherwise.} \end{cases}$$

The same scheme and number of points as in Example 1 and the CFL # = 0.9 were used. In Fig. 2a we plot the result at

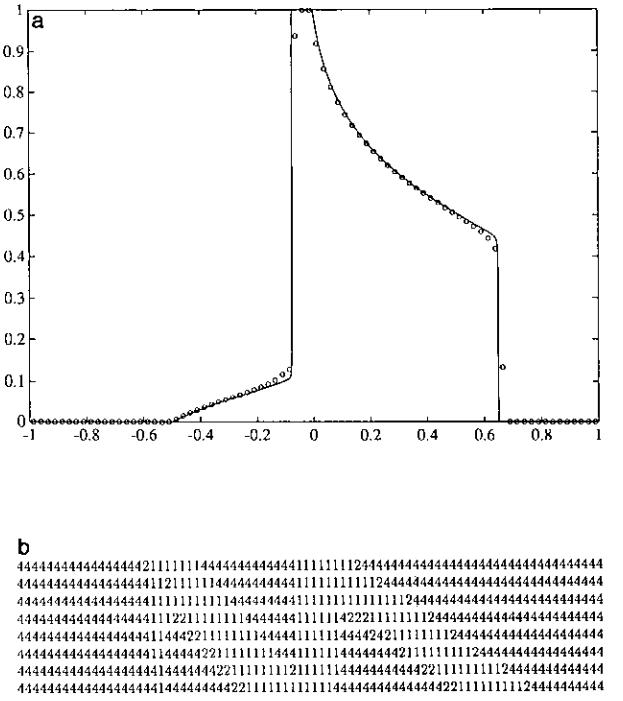

FIG. 2. The nonconvex problem of Example 2 computed with the variable order hybrid: (a) Computed solutions at $t = 0.4$ with 80 and 1000 points. (b) Schemes used at x_j for every second time step, as in Fig. 1.

time $t = 0.4$. The solid line represents a computation with 1000 points and is our approximation to the exact solution. In Fig. 2b we show the schemes used at each grid point for every five time steps.

2.3. *Switch Buffering*

Much simpler switching strategies can be designed which perform as well as or better than the variable order strategy described above. One point of view is that truncation error estimates or consistency tests as in (3) give means of *detecting* shocks (or other singularities). To minimize switching near singularities, it seems appropriate to *define* the shock zone, the zone in which the cheap scheme is not used, as those grid points sufficiently near any point where a shock was detected. To give a precise definition, suppose for example that we first determine initial switches as in (3),

$$\tilde{s}_j = \begin{cases} 0 & \text{if } |G_0(u^n)_j - G_1(u^n)_j| \leqslant \Delta t\, r(\Delta x) \\ 1 & \text{if } |G_0(u^n)_j - G_1(u^n)_j| > \Delta t\, r(\Delta x), \end{cases}$$

where we recall that G_1 is a monotone scheme and G_0 is arbitrary. For a given buffer size K, the final switches are defined as

$$s_j = \max_{|p| \leqslant K} \tilde{s}_{j+p}. \tag{12}$$

The shock zone is defined to consist of the set of grid points where $s_j = 1$. The hybrid can now be defined as in (2) and Theorem 1 still holds. In practice, simpler means of detecting shocks prove to be very effective, such as using smoothness indicators based on second or fourth differences. (Extensive use has been made of such indicators in the past, see [13, 12].) For example, one could define the initial switches $\tilde{s}_j$ as

$$\tilde{s}_j = \begin{cases} 0 & \text{if } |(\Delta^2 u)_j| \leqslant C_1\, \Delta x^2 \\ 1 & \text{if } |(\Delta^2 u)_j| < C_1\, \Delta x^2 \end{cases} \tag{13}$$

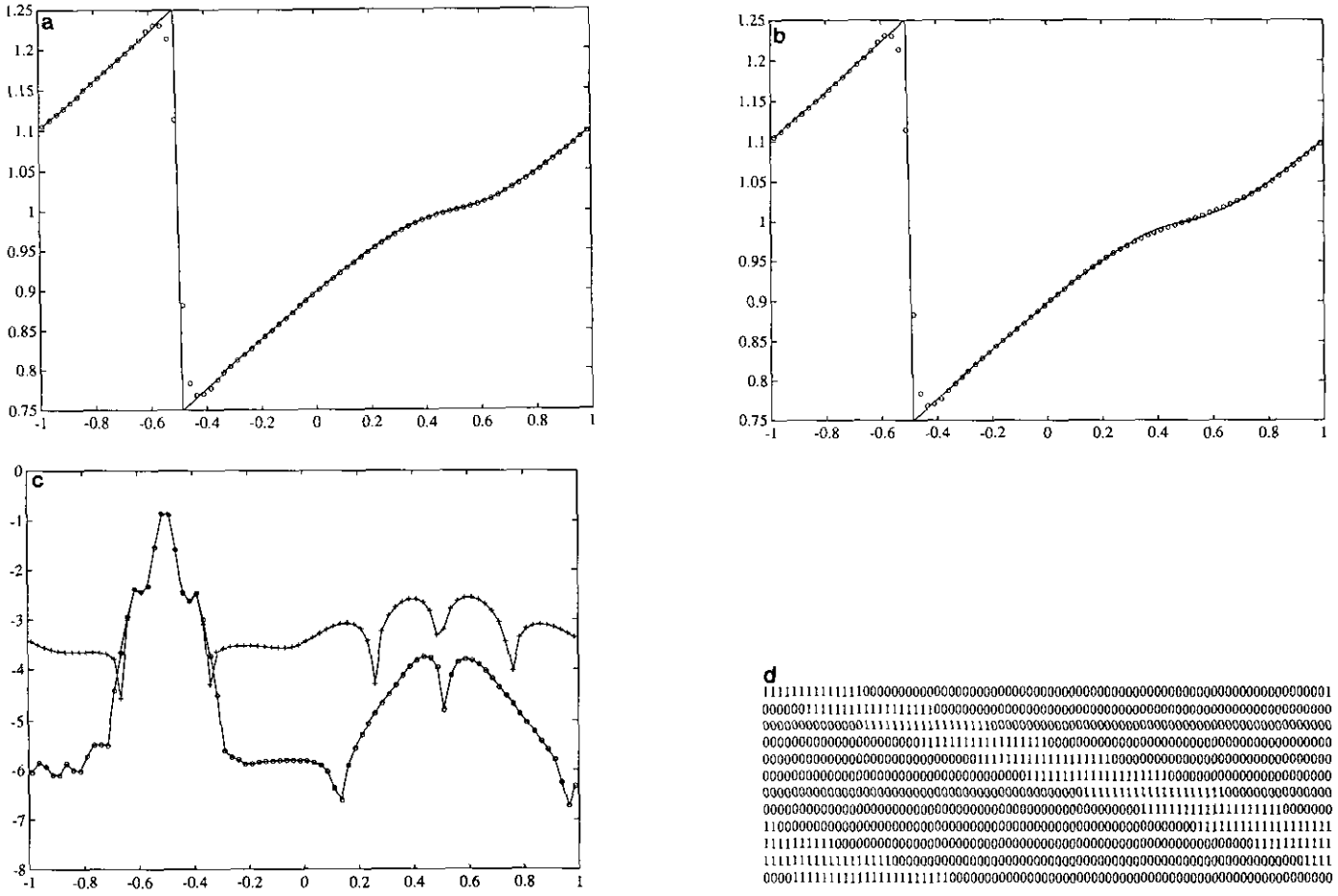

FIG. 3. Shock with a feature for Burgers' equation, computed with the switch buffering hybrid of Example 3: (a) Computed and exact solutions at $t = 2.5$. (b) The second-order Engquist–Osher scheme alone. (c) $\log_{10} |u_j - u(x_j)|$ at $t = 2.5$ for: O = Hybrid scheme from (a); + = second-order Engquist–Osher alone, from (b). (d) Schemes used by the hybrid for every 10th time step: 1 = second-order Engquist–Osher; 0 = fourth-order centered in x, Runge–Kutta in t.

or

$$\tilde{s}_j = \begin{cases} 0 & \text{if } |(\Delta^4 u)_j| \leqslant C_2 \Delta x^4 \\ 1 & \text{if } |(\Delta^4 u)_j| > C_2 \Delta x^4, \end{cases} \tag{14}$$

where $(\Delta^2 u)_j$, $(\Delta^4 u)_j$ are, respectively the second and fourth differences of u in space.

The "switch buffer" strategy indicated in (12) can virtually eliminate the error in shock speeds due to loss of conservation. The reason for this is that the switching is minimized and occurs inside the smooth region. Buffering can create a wide shock zone, though, so to achieve high resolution inside the shock zone a good shock capturing scheme is needed such as a MUSCL or ENO scheme.

Our suggested approach to hybrid construction allows great flexibility in selecting efficient and accurate schemes in smooth regions independently of the scheme used to treat shocks or other singularities. For example, the scheme used in Examples 3–6 below hybridizes G_{EO} = second-order Engquist–Osher scheme and G_{RK} = fourth-order centered differences in space with the classical Runge–Kutta time discretization. But we take advantage of the fact that for smooth solutions G_{RK} is stable for CFL numbers about double the largest stable CFL number permitted by G_{EO}. The computations are performed using a CFL # = 1.6 for G_{RK} and taking two "half" time steps with G_{EO} in shock zones, with CFL # = 0.8. The resulting scheme is therefore a hybrid defined by (2) with the schemes $G_0 = G_{RK}$ and $G_1 = G_{EO} \circ G_{EO}$. Half the computational effort is saved in smooth regions, at perhaps some cost in accuracy. But perhaps also it is better to gain some accuracy in the shock zone to balance resolution overall.

EXAMPLE 3. We consider the problem in Example 1. The scheme used is the hybrid just described, with switching based on fourth differences according to (14) and (12). The size of the buffer in (12) is chosen to be $K = 3$ and the constant in (14) is $C_2 = 500$. The results are not sensitive to small changes in these parameters. The result is shown in Fig. 3a. For comparison, in Fig. 3b the result for the single second-order Engquist–Osher scheme G_{EO} alone is shown. In Fig. 3c we plot the base 10 log of the error for the hybrid compared to that for G_{EO} alone. The schemes used at each grid point by the hybrid for every 10 time steps are shown in Fig. 3d, where $1 = G_{EO}$ and $0 = G_{RK}$.

Comparing with the variable order scheme (Fig. 1), we note the slightly better performance behind the shock with the switch buffer scheme. We found that this performance difference grows if the computation is continued until the shock becomes weak ($t = 15$ or so). With the variable order scheme, one begins to observe frequent switching at points in the shock zone and some consequent loss of accuracy in the position of the weak shock. With the switch buffer scheme, the shock eventually becomes smoothed out and too small to detect by (14), but G_{RK} continues to track its location accurately.

EXAMPLE 4. We consider the problem in Example 2 and the same hybrid as in Example 3. The results are shown in Fig. 4.

EXAMPLE 5. We consider the linear advection equation

$$u_t + u_x = 0$$

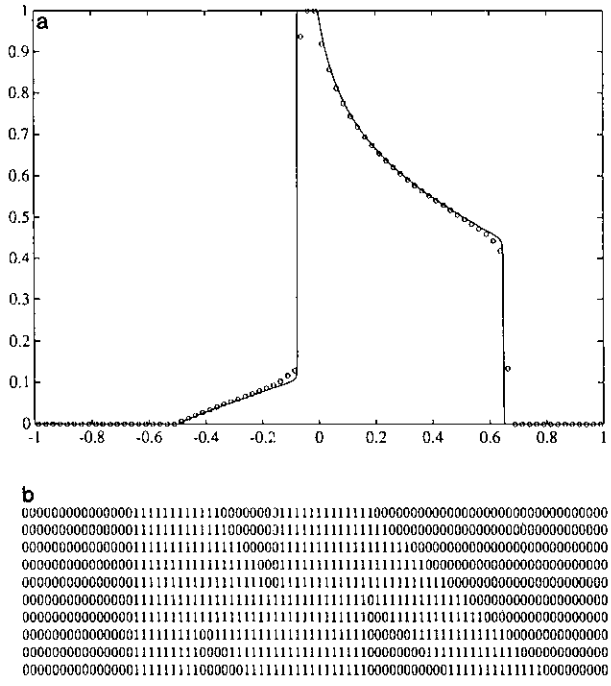

FIG. 4. The nonconvex problem computed with the switch buffering hybrid: (a) Computed solutions at $t = 0.4$ with 80 and 1000 points. (b) Schemes used at x_j for every second time step, as in Fig. 3.

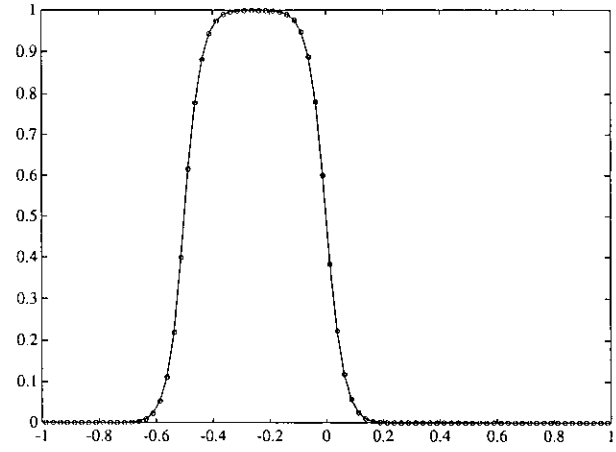

FIG. 5. Linear advection of a step function after one period, computed with the switch buffering hybrid.

with initial values as in Example 2. The same hybrid as in Example 3 is used and the result after one period is shown in Fig. 5.

EXAMPLE 6. (Systems—gas dynamics.) We consider the Riemann problem in one-dimensional gas dynamics. This is a system of three equations in the variables ρ, ρu, ρE denoting the density, momentum, and total energy, respectively (cf. [6]),

$$\rho_t + (\rho u)_x = 0$$
$$(\rho u)_t + (\rho u^2 + p)_x = 0$$
$$(\rho E)_t + (\rho u E + u p)_x = 0,$$

where the pressure p is obtained from $E = p/(\gamma - 1)\rho + u^2/2$, $\gamma = 1.4$, which is the equation of state for a polytropic gas (cf. [6]).

We first consider the initial values proposed by Sod:

$$(\rho, \rho u, \rho E)(x, 0) = \begin{cases} (1, 0, 2.5), & x < 0.5 \\ (0.125, 0, 0.250), & x > 0.5. \end{cases}$$

For G_1 the second-order TVD scheme based on the Roe solver denoted by G_{ROE2} is used, with CFL $\# \approx 0.8$. The second-order accuracy is achieved by adding a limited amount of antidiffusion to the first-order entropy-fixed Roe

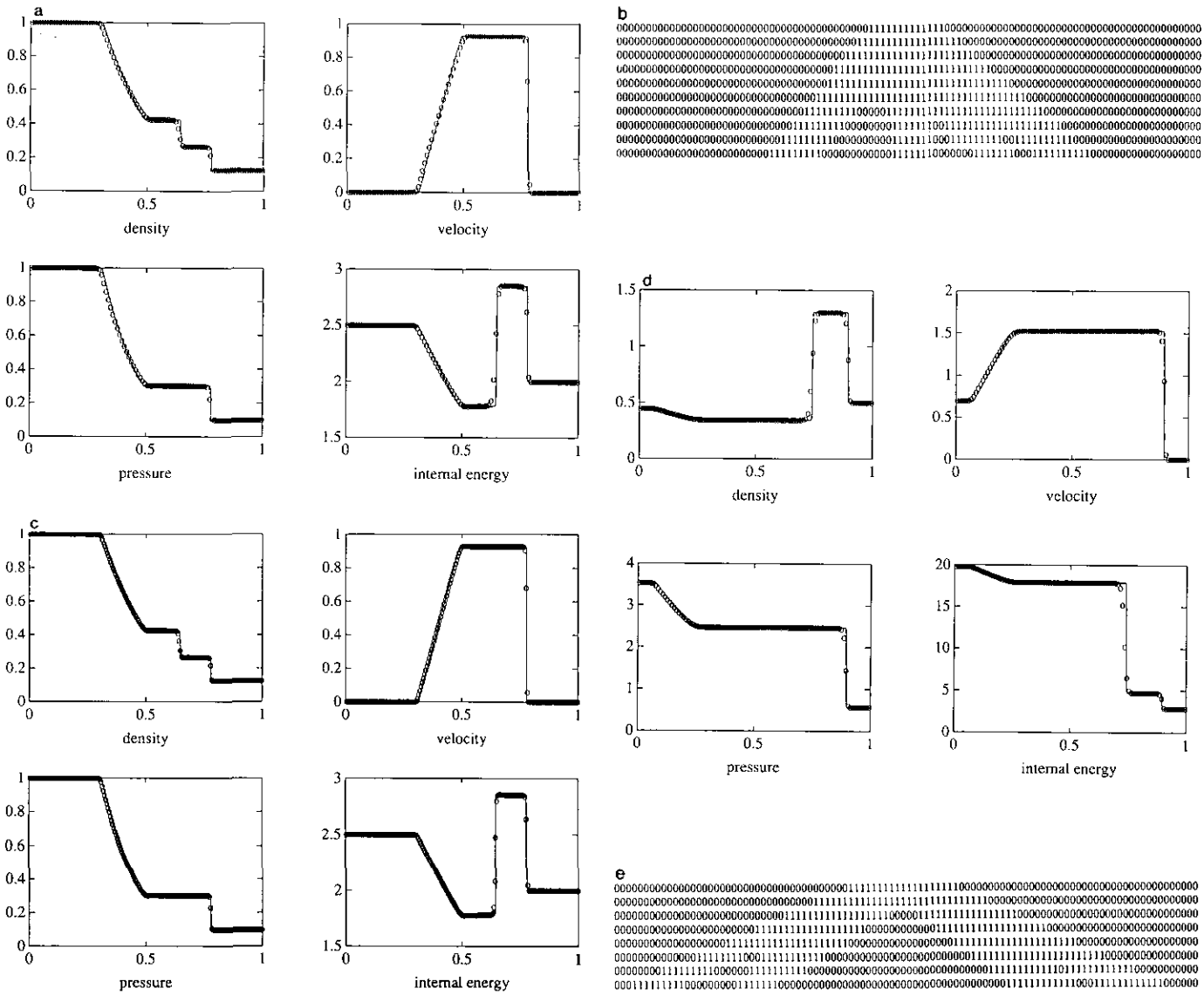

FIG. 6. The Riemann problem for gas dynamics with Sod's initial values and 100 points, computed with the switch buffering hybrid of Example 6: (a) Computed solution at $t = 0.16$ with 100 points. (b) Schemes used in (a) for every second time step: 1 = second-order Roe scheme; 0 = fourth-order centered in x, Runge–Kutta in t. (c) Computed solution at $t = 0.16$ with 200 points. The Riemann problem for gas dynamics with Harten's initial values and 100 points, computed with the switch buffering hybrid of Example 6: (d) Computed solution at $t = 0.16$ with 100 points. (e) Schemes used in (d) for every second time step: 1 = second-order Roe scheme; 0 = fourth-order centered in x, Runge–Kutta in t.

scheme (cf. [9, 19]). The overcompressive "superbee" limiter is used in the contact field for capturing sharp contact discontinuities. In the genuinely nonlinear fields the Chakravarthy–Osher limiter is used [19].

For G_0 the fourth-order accurate G_{RK} with a CFL # ≈ 1.6—twice the CFL number of G_{ROE2}— is used. Thus two "half" time steps are taken in shock zones as in Examples 3–5. Switching is based on second differences of the control variable ρE (replacing u in (13) by ρE), which permits one to detect the different types of singularities in the flow, i.e., shocks, contacts, and rarefaction corners.

The size of the buffer K is chosen to be three and the constant C_1 in (13) to be 1000/7. The algorithm is programmed efficiently, i.e., the expensive scheme G_{ROE2} is computed only when necessary, which is at relatively few points.

In Fig. 6a the solution at time $t = 0.16$ (20 time steps) with 100 points is shown. The solid line represents the solution computed with G_{ROE2} and 1000 points. The schemes used at each grid point for every two time steps is shown in Fig. 6b. The detection of singularities in the flow is marked by occurrences of ones, i.e., the points where G_{ROE2} was used. In Fig. 6c the solution with 200 points is shown.

Second, we consider the initial values proposed by Harten:

$$(\rho, \rho u, \rho E)(x, 0) = \begin{cases} (0.445, 0.311, 8.928), & x < 0.5 \\ (0.5, 0, 1.427), & x > 0.5. \end{cases}$$

The same hybrid and same parameters as in Sod's case are used. The result at $t = 0.16$ with 100 points is shown in Fig. 6d and the schemes at each grid point are used in Fig. 6e.

The results in Example 6 indicate that the nonconservative G_{ROE2}–G_{RK} hybrid tracks the discontinuities as well as the G_{ROE2} scheme alone (cf. [9, 19]). I.e., the lack of full conservation form does not appear to create significant error in the shock positions.

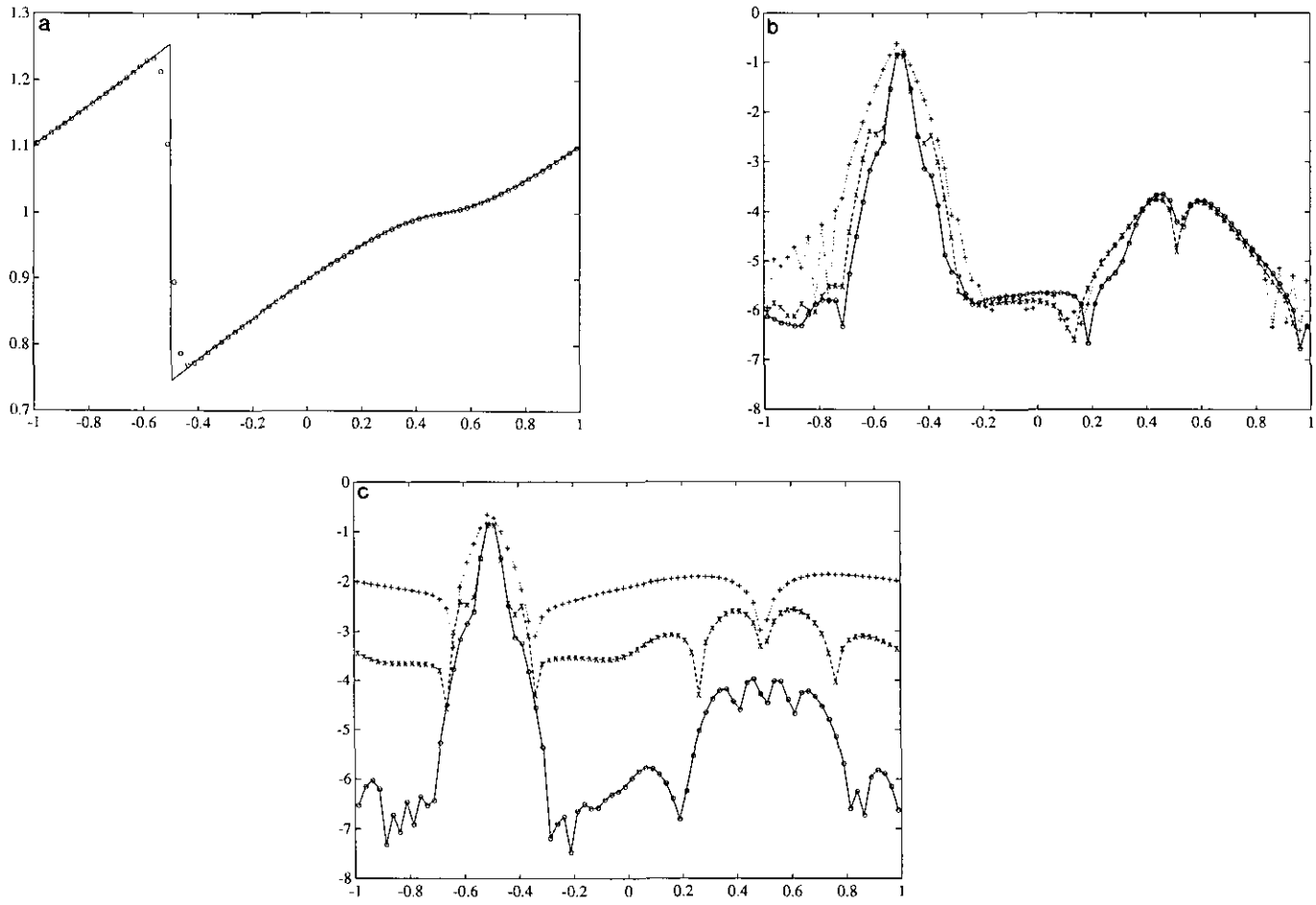

FIG. 7. Shock with a feature for Burgers' equation computed with the semidiscrete hybrid of Example 7: (a) Computed and exact solutions at $t = 2.5$. (b) $\log_{10} |u_j - u(x_j)|$ at $t = 2.5$ for three hybrid schemes: O = semidiscrete scheme from (a); × = second-order Engquist–Osher—fourth-order centered in x, RK in t; + = first-order Engquist–Osher—fourth-order centered in x, RK in t. (c) $\log_{10} |u_j - u(x_j)|$ at $t = 2.5$ for three pure schemes: O = Shu–Osher ENO in x, Runge–Kutta in t; × = second-order Engquist–Osher scheme; + = first-order Engquist–Osher scheme.

2.4. *Semidiscrete Hybrids*

From the programming viewpoint, it can be simpler to construct hybrids starting from two semi-discrete schemes

$$\frac{du_j}{dt} = K_0(u)_j, \qquad \frac{du_j}{dt} = K_1(u)_j.$$

Determine switches using a smoothness indicator as in (14) and a buffer as in (12) and solve

$$\frac{du_j}{dt} = K_H(u)_j = K_0(u)_j\,(1 - s_j) + K_1(u)_j\, s_j \qquad (15)$$

by an appropriate time discretization method. Here the switches are taken to be determined at each instant of time by u. Alternatively, one could compute the switches at discrete times t_n (perhaps every time step, perhaps less often) and keep them fixed on the time interval $t_n < t < t_{n+1}$.

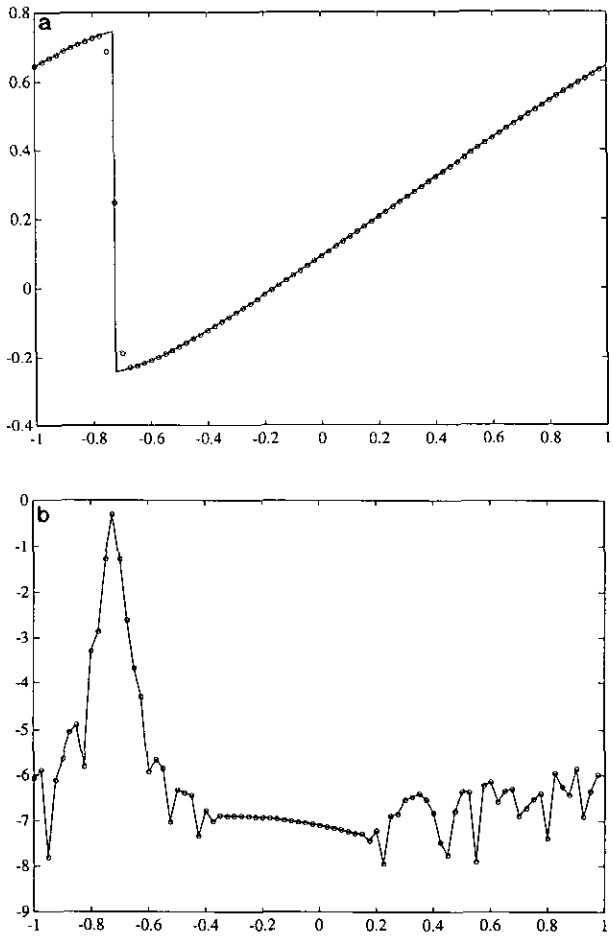

FIG. 8. Shock formation for Burgers' equation computed with the semidiscrete hybrid as in Example 8: (a) Computed and exact solutions at $t = 1.1$. (b) $\log_{10} |u_j - u(x_j)|$ at $t = 1.1$.

EXAMPLE 7. We compute the shock with feature considered in Example 1. We use the schemes K_0 = fourth-order centered differences in space, K_1 = semidiscrete fourth-order flux-based ENO scheme of Shu and Osher [18], which will be described in detail in the next section below. For that scheme, the parameter α is chosen to be $\alpha = 2.5$. Equation (15) is solved by the classical Runge–Kutta method, with CFL $\# = 0.8$, determining the switches only at the begin ning of each time step. A small amount of fourth-order dissipation is added to the scheme K_0. The switches are computed by (14) with $C_2 = 5 \times 10^3$ and (12) with $K = 3$. We plot u vs x in Fig. 7a. The base 10 log of absolute error is plotted in Fig. 7b, marked by circles. To compare similar hybrids that use different schemes in the shock zone, we also plot in Fig. 7b the results from Example 3 (marked by crosses), the hybrid of the second-order Engquist–Osher scheme, and the centered in space, Runge–Kutta in time scheme, and also (marked by plusses), the result from replacing the second-order Engquist–Osher scheme in Example 3 by the first-order Engquist–Osher scheme. In Fig. 7c the results of using the shock capturing schemes alone appear: Shu–Osher (ENO) scheme (circles), second-order Engquist–Osher (crosses), first-order Engquist–Osher (plusses).

EXAMPLE 8. Consider the inviscid Burgers equation as in Example 1 with periodic initial conditions

$$u(x, 0) = \tfrac{1}{4} + \tfrac{1}{2} \sin \pi x. \qquad (16)$$

The exact solution is smooth initially, then develops a shock at $t = 2/\pi$ which lies on the line $x = -1 + t/4$. We use the same scheme as in Example 7, without fourth-order dissipation and with $\alpha = 1.2$. The CFL $\# = 0.6$, and $C_2 = 5 \times 10^3$, $K = 3$. At $t = 1.1$ we plot the solution in Fig. 8a and the base 10 log of the error in Fig. 8b.

3. A HYBRID IN CONSERVATION FORM

The main point of this section is to construct an efficient hybrid scheme based on a numerical flux which switches from that for a fourth-order centered difference scheme to a fourth-order ENO flux, which is a modification of a flux-based scheme of Shu and Osher [18]. The hybrid retains full fourth-order formal accuracy both at extrema and at points where switching occurs.

First, however, we describe a general way of constructing hybrid schemes in conservation form by exploiting an idea of Shu and Osher [18]. Related ideas have also been developed by Cockburn [3]. Shu and Osher construct a numerical flux which they observe is a $O(\Delta x^2)$ perturbation of the numerical flux of a TVD (total variation diminishing) scheme and, hence, yields a TVB (total variation bounded)

scheme. Our line of thought now suggests that *any* given conservation form scheme can be made TVB by hybridizing appropriately with a TVD scheme. For example, suppose we are given an arbitrary conservation form scheme

$$u_j^{n+1} = G(u^n)_j = u_j^n - \lambda(\hat{f}_{j+1/2} - \hat{f}_{j-1/2}), \tag{17}$$

where $\lambda = \Delta t/\Delta x$, with a consistent numerical flux,

$$\hat{f}_{j+1/2} = \hat{f}(u_{j-l}, ..., u_{j+k}), \qquad \hat{f}(u, ..., u) = f(u), \tag{18}$$

and a TVD numerical flux $\hat{f}^{\mathrm{TVD}}$, and a constant M. Then we can define a hybrid scheme using the "switch buffering" idea of Section 2.4 as follows: Define switches $\tilde{s}_{j+1/2}$ by

$$\tilde{s}_{j+1/2} = \begin{cases} 0 & \text{if } |\hat{f}_{j+1/2} - \hat{f}^{\mathrm{TVD}}_{j+1/2}| \leqslant M\,\Delta t\,\Delta x \\ 1 & \text{if } |\hat{f}_{j+1/2} - \hat{f}^{\mathrm{TVD}}_{j+1/2}| > M\,\Delta t\,\Delta x. \end{cases} \tag{19}$$

Let a buffer width K be given and define

$$s_{j+1/2} = \max_{|p| \leqslant K} \tilde{s}_{j+p+1/2}. \tag{20}$$

Then define the hybrid flux by

$$\hat{f}^{\mathrm{HY}}_{j+1/2} = \hat{f}_{j+1/2} + s_{j+1/2}(\hat{f}^{\mathrm{TVD}}_{j+1/2} - \hat{f}_{j+1/2}). \tag{21}$$

A precise result on the total variation bound for a scheme defined as in (19)–(21) will be presented in Theorem 2. From a practical point of view, however, such a scheme has the drawback that both fluxes must be computed at every grid point in order to set the switches. Thus if the TVD scheme is expensive to compute, this scheme has little point. As we discussed in Section 2, a more practical way of setting the initial switches $\tilde{s}_{j+1/2}$ would be to use a smoothness indicator as in (13) or (14). A numerical experiment with a scheme of this sort will be presented below.

THEOREM 2. *Assume the scheme G is a TVD scheme with a finite stencil of width $2P+1$, and the scheme G_H satisfies*

$$|G_H(u)_j - G(u)_j| \leqslant M\,\Delta t\,\Delta x$$

for all j, for some constant M, for any bounded grid function u. Assume $\Delta t/\Delta x \geqslant c_0 > 0$. Then G_H is a locally TVB scheme: If $u_j^{n+1} = G_H(u^n)_j$ for $n = 0, 1, ...$ then so long as $n\,\Delta t \leqslant T$ and $(2q+1)\,\Delta x \leqslant L$, we have

$$\sum_{|j| \leqslant q} |u^n_{j+l} - u^n_j| \leqslant \sum_{|j| \leqslant q+nP} |u^0_{j+l} - u^0_j| + C(T, L)M, \tag{22}$$

where $C(T, L) = 2T(L + 2PT/c_0)$.

Proof. We have

$$\begin{aligned} \sum_{|j| \leqslant q} |u^n_{j+1} - u^n_j| &= \sum_{|j| \leqslant q} |G_H(u^{n-1})_{j+1} - G_H(u^{n-1})_j| \\ &\leqslant \sum_{|j| \leqslant q} |G(u^{n-1})_{j+1} - G(u^{n-1})_j| \\ &\quad + (2q+1)\,2M\,\Delta t\,\Delta x. \end{aligned}$$

Define

$$\tilde{u}_j = \begin{cases} u^{n-1}_{q+P} & \text{for } j > q+P \\ u^{n-1}_j & \text{for } |j| \leqslant q+P \\ u^{n-1}_{-q-P} & \text{for } j < -q-P. \end{cases}$$

Then $G(\tilde{u})_j = G(u^{n-1})_j$ for $|j| \leqslant q$ and we have

$$\begin{aligned} \sum_{|j| \leqslant q} |G(\tilde{u})_{j+1} - G(\tilde{u})_j| &\leqslant \sum_j |G(\tilde{u})_{j+1} - G(\tilde{u})_j| \\ &\leqslant \sum_j |\tilde{u}_{j+1} - \tilde{u}_j| \\ &\leqslant \sum_{|j| \leqslant q+P} |u^{n-1}_{j+1} - u^{n-1}_j|. \end{aligned}$$

The estimate (22) now follows by induction.

A practical useful hybrid scheme should have certain characteristics: It should employ an inexpensive, accurate scheme outside shock zones and a high quality shock-capturing scheme inside shock zones. In a conservative hybrid such as we have described, it is desirable to have the two schemes compatible, to avoid loss of accuracy at the point where switching occurs. Here we describe how a high quality fourth-order ENO scheme of Shu and Osher may be modified so that it may be hybridized with a fourth-order centered difference scheme while avoiding loss of accuracy when switching in smooth regions. The hybrid scheme retains full fourth-order formal accuracy for smooth solutions.

The particular scheme of Shu and Osher which we discuss originates from a semidiscrete scheme of the form

$$\frac{du_j}{dt} = -\frac{1}{\Delta x}(\hat{f}_{j+1/2} - \hat{f}_{j-1/2}). \tag{23}$$

The forward Euler method applied to (23) yields (17). If this scheme were TVD, the ODEs in (23) can be solved by Runge–Kutta methods designed to produce a TVD scheme [18]. The construction of $\hat{f}$ is designed to yield a truncation error estimate of order $2m$ for f_x,

$$f(u(x))_x = \frac{1}{\Delta x}(\hat{f}_{j+1/2} - \hat{f}_{j-1/2}) + O(\Delta x^{2m}). \tag{24}$$

For stability reasons, this will be achieved through separate approximations $\hat{f}^+$ and $\hat{f}^-$ corresponding to

$$f^+(u) = \tfrac{1}{2}(f(u) + \alpha u),$$
$$f^-(u) = \tfrac{1}{2}(f(u) - \alpha u),$$

where $\alpha \geqslant \max |f'(u)|$ is a constant. (The stencils for $\hat{f}^+$ and $\hat{f}^-$ are determined differently.) Let $f_{j+1/2}$ denote $f(u(x_{j+1/2}))$ and $f|_{j-1/2}^{j+1/2}$ denote $f_{j+1/2} - f_{j-1/2}$. Shu and Osher observe that if $a_2 = -\frac{1}{24}$, $a_4 = \frac{7}{5760}$, etc., then

$$\left(\frac{\partial}{\partial x} f\right)_j = \frac{1}{\Delta x}\left[f + \sum_{k=1}^{m-1} a_{2k}\, \Delta x^{2k} \frac{\partial^{2k}}{\partial x^{2k}} f\right]_{j-1/2}^{j+1/2} + O(\Delta x^{2m}). \tag{25}$$

They therefore define polynomial interpolants $p_{j+1/2}^{\pm}$ of order $2m$ interpolating $f^{\pm}$ at $2m+1$ points near $x_{j+1/2}$ (chosen according to ENO ideas), from which it follows that

$$\Delta x^k \frac{\partial^k}{\partial x^k} p_{j+1/2}^{\pm}(x) = \Delta x^k \frac{\partial^k}{\partial x^k} f^{\pm}(u(x)) + O(\Delta x^{2m+1})$$

for $k = 0, 1, \ldots, 2m$. Then the numerical flux is defined by $\hat{f} = \hat{f}^+ + \hat{f}^-$, where

$$\hat{f}_{j+1/2}^{\pm} = \left[p_{j+1/2}^{\pm} + \sum_{k=1}^{m-1} a_{2k}\, \Delta x^{2k} \frac{\partial^{2k}}{\partial x^{2k}} p_{j+1/2}^{\pm}\right]_{x = x_{j+1/2}}. \tag{26}$$

The truncation error estimate (24) is therefore achieved.

Let us consider the case $m = 2$ and compare with the numerical flux for fourth-order centered differences. That flux is

$$\hat{f}_{j+1/2}^{C} = (-f_{j+2} + 7f_{j+1} - 7f_j + f_{j-1})/12. \tag{27}$$

Hybridizing this flux with the ENO flux yields only third-order accuracy, unfortunately, since for example, from (25)–(26) it follows that

$$\begin{aligned}
&\frac{1}{\Delta x}(\hat{f}_{j+1/2}^{C} - \hat{f}_{j-1/2}) \\
&\quad = \frac{1}{\Delta x}\left[f_{j+1/2} - \frac{1}{24}\Delta x^2 f''_{j+1/2}\right. \\
&\qquad - \frac{37}{1152}\Delta x^4 f^{(4)}_{j+1/2} + O(\Delta x^6) \\
&\qquad \left. - \left(f_{j-1/2} - \frac{1}{24}\Delta x^2 f''_{j-1/2} + O(\Delta x^5)\right)\right] \\
&\quad = \left(\frac{\partial}{\partial x} f\right)_j + O(\Delta x^3).
\end{aligned} \tag{28}$$

However, since $f^{(4)}_{j+1/2} - f^{(4)}_{j-1/2} = O(\Delta x)$ for smooth solutions, full fourth-order accuracy in (28) can be recovered if we take Shu and Osher's scheme and simply modify (26) in the case $m = 2$ by adding the appropriate term of order $O(\Delta x^4)$, obtaining

$$\hat{f}_{j+1/2}^{\pm} = \left[p_{j+1/2}^{\pm} - \frac{1}{24}\Delta x^2 \frac{\partial^2}{\partial x^2} p_{j+1/2}^{\pm} - \frac{37}{1152}\Delta x^4 \frac{\partial^4}{\partial x^4} p_{j+1/2}^{\pm}\right]_{x = x_{j+1/2}}. \tag{29}$$

The resulting pure ENO scheme also retains formal fourth-order accuracy, including at extreme points. (On a related point, note that if the coefficient $-37/1152$ in (29) is replaced by $a_4 = 7/5760$, the resulting pure ENO scheme is formally fifth-order accurate, assuming the stencil is fixed. But when the stencil does change, this scheme is formally only fourth-order accurate, and the extra term does not increase the accuracy of the scheme in (25) and (26).)

EXAMPLE 9. We consider the same test problem as Example 8. We use a conservative hybrid scheme switching between the flux $\hat{f}^C$ in (27) and the ENO flux of Shu and Osher determined from (26), with and without the modification in (29). Switches are comuted from fourth differences as in (14), (12) with $C_2 = 5 \times 10^3$, $K = 10$. The base 10 log of the error is plotted in Fig. 9a, marked with crosses (unmodified) or circles (modified). In general, we observed little difference in the results produced by the hybrid scheme with and without the modification. To see some difference, a wide buffer seems to be required, as in the calculation shown. A slight improvement is seen with the modification. With a practical buffer size, the larger error at switching points produced by the unmodified scheme may be too near

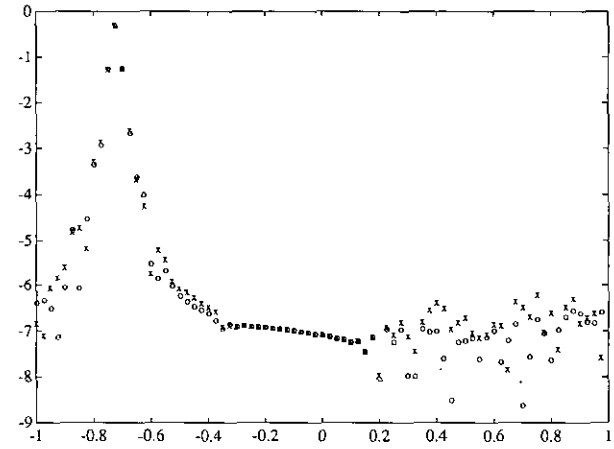

FIG. 9. Shock formation for Burgers' equation computed with conservative flux switching, $\log_{10}|u_j - u(x_j)|$ for the hybrid schemes: ○—modified fourth-order Shu–Osher ENO—fourth-order centered; ×—unmodified fourth-order Shu–Osher—fourth-order centered.

the shock to be significant or may be suppressed by the focussing of characteristics toward the shock in one dimension. It is interesting, however, to note that the nonconservative hybrid of Example 8 (see Fig. 8b) yields results comparable to the conservative hybrids.

4. CONCLUSIONS

In this paper we have constructed simple, efficient, and accurate nonconservative hybrids based on several switching strategies. When switching occurs between two accurate conservative schemes only in smooth regions, the error in shock speeds due to loss of conservation form is virtually eliminated. The switching strategies which are most successful in practice have the key feature that they distinguish between *detecting* and *defining* the shock zone, i.e., between locating singularities and choosing an appropriate scheme to deal with them. In particular, the strategy of nonconservative switching described in Section 2.3, based on detecting shocks with a smoothness indicator, but incorporating a "buffer" in the shock zone definition, provides great flexibility in selecting efficient and accurate schemes for smooth regions independently of the sophisticated scheme used to treat shocks or other singularities.

Thus, for example, it should not be a great task to modify an existing high quality one-step shock-capturing code to form a hybrid with a centered-in-x, RK-in-t scheme (provided the grid geometry is regular, at least). Once switches have been determined, simply testing whether a switch is 0 or 1 could save the cost of computing the expensive scheme in smooth regions. And the cheap scheme may be vectorizable, since the schemes can be computed independently over each time step. Vectorization would have the trade-off (slight, one hopes) that values computed in the shock zone would be discarded, however.

Along with difficulty in programming, another traditional drawback associated with hybrid schemes has been the "nonintrinsic" nature of smoothness indicators such as those we use in (13) and (14), sometimes requiring a delicate problem-dependent choice of parameters to achieve good results. We have no general remedy for this problem but have indicated how the switch buffer strategy helps reduce the ill effects of the sometimes irregular pattern generated by such detectors. Also, our experience is that the test based on fourth differences in (14) is much less sensitive to the choice of parameter that the test in (13).

One possibility which has not been discussed before, but which may be of practical value, is to use a locally refined mesh in the shock zone. One of the difficulties addressed in earlier work [1]—achieving conservation form at the interface between coarse and fine mesh zones—might be eliminated by using a nonconservative switching strategy such as we have described, to make sure that grid interfaces occur in smooth regions.

Finally, we mention that the ultimate utility of the ideas we have described probably depends on what efficiency gains can be achieved in multidimensional shock computations. Unfortunately, we have not been able to address this issue in the present paper, feeling that it is better it be addressed by those with more experience with large scale computations.

REFERENCES

1. M. Berger, *SIAM J. Num. Anal.* **24**, 967 (1987).
2. S. R. Chakravarthy, A. Harten, and S. Osher, "Essentially Non-oscillatory Shock-Capturing Schemes of Arbitrarily High Accuracy," AIAA 24th Aerospace Sciences Meeting, Reno, Nevada, Jan. 6–9, 1986.
3. B. Cockburn, *SIAM J. Num. Anal.* **26**, 1325 (1989).
4. B. Cockburn and C.-W. Shu, *Math. Comput.* **52**, 411 (1989).
5. P. Colella and P. R. Woodward, *J. Comput. Phys.* **54**, 174 (1984).
6. R. Courant and K. O. Friedrichs, *Supersonic Flow and Shock Waves* (Springer-Verlag, New York, 1976).
7. M. Crandall and A. Majda, *Math. Comput.* **34**, 1 (1980).
8. B. Engquist, P. Lötstedt and B. Sjögreen, *Math. Comput.* **52**, 509 (1989).
9. A. Harten, *J. Comput. Phys.* **49**, 357 (1983).
10. A. Harten, B. Engquist, S. Osher, and S. R. Chakravarthy, *J. Comput. Phys.* **71**, 231 (1987).
11. A. Harten and S. Osher, *SIAM J. Num. Anal.* **24**, 279 (1987).
12. A. Harten and G. Zwas, *J. Comput. Phys.* **9**, 568 (1972).
13. A. Jameson, *Commun. Pure Appl. Math.* **41**, 507 (1988).
14. A. Y. LeRoux, *RAIRO Anal. Numer.* **15**, 151 (1981).
15. S. Osher and S. Chakravarthy, *SIAM J. Num. Anal.* **21**, 955 (1984).
16. R. Sanders, *Math. Comput.* **51**, 535 (1988).
17. C.-W. Shu, *Math. Comput.* **49**, 105 (1987).
18. C.-W. Shu and S. Osher, *J. Comput. Phys.* **77**, 439 (1988).
19. P. K. Sweby, *SIAM J. Num. Anal.* **21** (1984).
20. B. van Leer, *Lect. Notes in Phys., Vol. 18* (Springer-Verlag, New York/Berlin, 1973), p. 163.
21. B. van Leer, *J. Comput. Phys.* **14**, 361 (1974).